Motion Planning for Autonomous Grain Carts

Lantian Shangguan, J. Alex Thomasson, and Swaminathan Gopalswamy

***Abstract*—When harvesting grain crops on large farms, a combine collects the grain while a grain cart transports the grain by commuting between the combine and a semi-trailer parked by the roadside. There are several issues associated with human-operated grain carts: labor shortage and increasing labor cost, operational imprecision and inefficiency as well as safety hazards, all of which can potentially be addressed if grain carts were autonomous. This paper presents a motion planning algorithm and the associated navigation solution for autonomous grain carts. The algorithm features a novel integration of Artificial Potential Field (APF) with Fuzzy Logic Control (FLC). A set of simulation tests were carried out, comparing the proposed APF+FLC planner with a simple APF planner. The test results verified the effectiveness, robustness, and efficiency of the proposed planning algorithm in performing the logistical tasks in harvest operations where unharvested crops were the only obstacles as well as when random static or dynamic obstacles existed. In addition, a set of mobile robot tests implementing the proposed navigation solution were conducted, in which the robot representing the grain cart autonomously accomplished the logistical tasks in the harvest operations, verifying the effectiveness and practicality of the navigation solution.**

***Index Terms*—Motion planning, autonomous grain carts, navigation solution, Artificial Potential Field, Fuzzy Logic Control.**

I. Problem Definition

WHEN harvesting grain crops such as wheat, soy, rice and corn, a combine follows a specific route to cover the field while a grain cart towed by a tractor performs a series of supporting logistical tasks. When the combine's tank fills up, the grain cart will approach and drive alongside the combine to unload the grain without interrupting harvesting. Then the grain cart will travel to an in-field storage station, which is typically a semi-trailer parked by the roadside for later road transport. After transferring the grain to the semi-trailer, the grain cart will get prepared for the next work cycle. All the grain-cart operations are currently executed by a human tractor driver. However, finding and keeping skilled farm laborers to perform such tasks is becoming a greater challenge, and labor costs are increasing [1]. Even with higher wages, few American workers are attracted to farm labor, as it can be difficult and physically demanding. Timely and fast harvesting is critical to minimizing field losses due to weather, so solutions are needed to mitigate the labor shortage. If grain carts were autonomous, they could potentially operate all day every day with no human operator. With a sophisticated navigation system (including sensing, control and actuation), autonomous grain carts could potentially "see," "think" and "act" with high precision and efficiency as well as enhanced operational safety. While humans have inherent limitations (e.g., reaction time, vision, fatigue, potential impairments such as alcohol) and could choose to operate improperly (e.g., take a shortcut or ignore a warning), autonomous grain carts could be equipped with blind-spot-free sensors and responsive actuators, and be programmed to never take risky actions. Providing nonstop operation with reduced labor and improved precision, efficiency and safety, autonomous grain carts could potentially bring about higher productivity and great economic benefits to agriculture.

A. Challenges

The objective in harvest is to maximize crop quantity and quality while minimizing the inputs of fuel, time and labor. Doing so requires the combine to operate nearly nonstop throughout the harvest, requiring the grain cart to meet the combine when the combine reaches full capacity. When meeting late, the combine may fill up and be forced to stop before the cart arrives, interrupting the harvesting; when meeting early, the grain cart may have to follow the combine before unloading starts, resulting in more fuel consumption and nonproductive time. This important meeting timing is currently determined by the combine's operator based on experience, which can be inconsistent and is often suboptimal [2]. In addition to the temporal constraints above, the dynamic nature of the harvesting environment makes motion planning for grain carts more complex. As a combine harvests the field, harvested areas that are traversable for the grain cart are constantly changing. Routes planned in the last work cycle could have become suboptimal and need updating. Moreover, only the track to the left of the combine's path can be used by the grain cart for unloading, as almost all combines have the unloading auger on the left. Besides temporal and spatial constraints, unexpected obstacles or events may occur during harvesting, such as the varying yield of different field areas that can change the combine's speed and fill rate, or another vehicle's passing through the field and interfering with the harvest. Thus motion planning for grain carts is inherently a dynamic problem that needs real-time adaptation. Furthermore, the numerous parameters associated with harvest operations contribute to the difficulty of this problem [3]: the combine's dimensions, pose,

Manuscript received May 2, 2020; revised October 22, 2020; accepted January 17, 2021. Date of publication February 9, 2021; date of current version April 2, 2021. The review of this article was coordinated by Dr. E. Velenis. *(Corresponding author: Lantian Shangguan.)*

Lantian Shangguan is with the Intelligent Vehicle Business Unit as part of the Intelligent Driving Group at Baidu, Inc., Shenzhen, Guangdong 518063, China (e-mail: sglt.nicholas@gmail.com).

J. Alex Thomasson is with the Department of Agricultural and Biological Engineering, Mississippi State University, Mississippi State, MS 39762 USA (e-mail: athomasson@abe.msstate.edu).

Swaminathan Gopalswamy is with the Department of Mechanical Engineering, Texas A&M University, College Station, TX 77843 USA (e-mail: sgopalswamy@tamu.edu).

Digital Object Identifier 10.1109/TVT.2021.3058274

speed, capacity, and fill rate; the field's geometry and yield; and the grain cart's dimensions, pose, speed, unloading rate and kinematic constraints.

B. Related Work

Numerous farming equipment manufacturers and startups have ongoing projects that involve autonomous agricultural vehicles (AAVs). To name a few recent projects or products related to harvesting and/or coordination of multiple vehicles, Case IH's vehicle-to-vehicle (V2V) system enables a combine to take control of the grain cart and coordinate both machines for more efficient cooperation; Machine Sync and AutoTrac by John Deere can, respectively, connect up to ten machines within three miles to synchronize their movements and automatically steer the machine through the field; Kinze is testing their autonomous harvesting system, which will allow combine operators to remotely coordinate grain carts via touch-screens; AGCO unveiled a prototype of GuideConnect, a system that pairs vehicles as a single unit to improve farming productivity; Autonomous Tractor Corporation has been engineering AutoDrive, a retrofit kit that will allow tractors to perform a variety of tasks after sufficient training; Case IH unveiled a cab-less autonomous concept tractor, which can be remotely supervised and controlled with a tablet; carrying the same technology as Case IH, New Holland's NHDrive maintains a fully equipped cab so a human operator can handle tasks too challenging for complete autonomy; Yanmar launched the Auto Tractor and the unmanned Robot Tractor, both of which can be operated by a tablet; Smart Ag released AutoCart, a cloud-based software application that allows farmers to use tablets to manipulate grain carts to service combines.

In parallel with efforts in industry, a number of academic studies involving planning for AAVs have been published. These studies can be categorized into (i) coordination of multiple agricultural vehicles, (ii) motion planning in complex agricultural environments, and (iii) task scheduling with temporal constraints. In the first category, many have been investigating leader-follower systems in which one unmanned vehicle follows another that is either manned or unmanned [4]–[7]. Some have researched and developed control frameworks to coordinate and synthesize teams of agricultural vehicles [8], [9]. In the second category, researchers have looked into optimized coverage planning for agricultural operations in the fields where obstacles are present [10], algorithmic approaches for optimal path generation for service units [11], and randomized rapid motion planning for mobile robots in agricultural environments [12]. In the third and final category, researchers have approached task scheduling from various perspectives. For example, one study provided insight into how time constraints on location of demands could be converted into an underlying reachability graph, based on which routing policies could be designed for a service vehicle [13]. Another study proposed two optimization methods that could provide optimal solutions to vehicle routing problems under time constraints with up to one hundred visiting points [14].

Most AAV systems being developed or marketed in industry (e.g., remote control, leader-follower, driving assistance) may be practical for today's farming operations, but they are better described as semi-autonomous instead of fully autonomous, as human supervision and control is still required. In academia, the majority of AAV studies solve simplified generic problems without focusing on specific farming operations that are often of higher complexity. The interactions between combines and automated grain carts that are characterized by tight interleaving of temporal and spatial constraints have been scarcely investigated [15]. Most production-level harvesting with combines and grain carts is still performed without detailed planning, and harvesting efficiency heavily relies on the operators' experience [2].

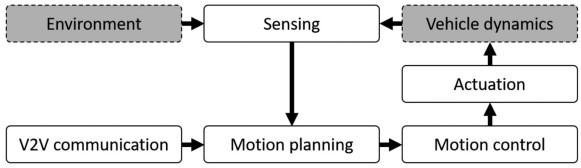

Fig. 1. General architecture of navigation systems on AAVs.

C. Objectives

To address the research gaps noted above, this study attempts to develop a motion planning algorithm to facilitate full autonomy of grain carts. This overall goal can be divided into the following two specific objectives. The first objective is to develop a motion planning algorithm and an associated task scheduling strategy for grain carts to autonomously navigate in the field and accomplish the logistical tasks in harvest operations, handling the spatial and temporal constraints. The solution procedure involves performing simulation tests to verify the effectiveness (i.e., accomplishment of logistical tasks), robustness (i.e., effectiveness in simple and complex test cases), efficiency (i.e., generation of short and smooth paths) and computational ease (i.e., low consumption of CPU time) of the motion planning algorithm. The second objective is to provide a high-level software and hardware solution to building navigation systems on autonomous grain carts for implementing the proposed motion planning algorithm. This objective covers sensor selection, communication options, control technique, and actuation plan. The solution procedure involves carrying out mobile robot tests to verify the effectiveness and practicality (i.e., effectiveness in physical setups) of the navigation solution.

II. Solution Procedure

A. Navigation Solution

This study accounts for the following technology components, which are indispensable to building an AAV: sensors that perceive the environment and measure the vehicle's states; communication between the vehicles for information sharing; decision-making algorithms for planning and control; and actuators for implementing the control commands. Fig. 1 illustrates a general architecture of navigation systems that can be extracted and summarized from other studies [5], [16]–[19]. Excluding the planner development, this subsection provides the technology background and high-level solution to building the navigation

system on an autonomous grain cart, covering sensor selection, communication options, control technique and actuation plan.

1) Sensor Selection. Global Localization: Extensively used in precision farming and agricultural automation, GPS-based systems can be adopted for localizing autonomous grain carts, which is required to be performed in real-time with centimeter-level accuracy as a grain cart needs to carefully cooperate with the combine in close proximity to unload the grain evenly and precisely into the cart. Fortunately, this can be achieved with RTK-GPS. Even if the rover receiver is as much as 10 km away from the base receiver, RTK-GPS can provide accuracy of 2 cm, fulfilling the localization requirement.

Local Perception: Real-time environmental awareness is essential not only for differentiating traversable harvested areas from unharvested areas, but also for detecting a variety of static obstacles (e.g., trees, utility poles and storage buildings) and potentially dynamic obstacles (e.g., people, animals and other farming machines) that can be encountered in the field. Considering the large scales of crop fields, autonomous navigation of grain carts would require a sensing range of hundreds of meters. Meanwhile, centimeter-level accuracy and resolution are needed so that obstacles like individual crop plants and utility poles would not be missed. Different alternatives for local perception are available, including monocular or stereo computer vision, radar, and lidar, but each has advantages and disadvantages. Lidar has drawn much attention recently for sensing on autonomous vehicles. Although it is somewhat sensitive to dust, fog and rain, lidar provides high accuracy, high resolution and fast detection over a reasonable range (up to 250 m). Reports from several studies [17], [18], [20] have discussed the superiority of lidar over other widely used sensors in robustness, range, response speed and cost in AAV applications. Considering that (i) most harvests take place in weather conditions without rain or fog, and (ii) the primary task of the grain cart is to navigate through crop rows (i.e., obstacle avoidance with no need for identification of traffic lights or signs), 2D lidar should be able to deliver sufficient local perception for an autonomous grain cart.

States Measurement: Real-time measurement of the grain cart's states of motion is also needed for planning and control. This can be realized by Inertial Measurement Units (IMUs). Error accumulation over time, the most notable problem with IMUs can be addressed by sensor fusion. For example, fluxgate compasses, magnetic counters and radar sensors can all be incorporated complementarily to IMUs for higher robustness and accuracy.

2) Communication Options: Establishment of V2V communication is imperative as the grain cart needs to know the combine's pose, speed and fill level for planning when and where to go for meeting. Cell Global System for Mobile communications (GSM) networks are known for their broad coverage and good signal quality, but they are far more expensive to establish and maintain than Wireless Local Area Network (WLAN). The WLAN transmission range can be extended to kilometers, and it consumes much less energy than GSM while providing a signaling rate high enough for fast transfers of video, audio, graphics and files. Consuming relatively minimal power, Bluetooth is commonly used for communication among relatively simple devices, transferring audio, graphics and files at 1 Mbps but only within very short distances (i.e., typically less than 10 m). Finally, ZigBee, featuring low bit rate (250 kbps), power consumption and latency as well as a simple network configuration, is suitable for small data packet transfer in wireless control and monitoring applications. The ZigBee transmission distance can also be enlarged to kilometers by establishing a mesh network with intermediate devices. The above comparison shows that WLAN and ZigBee meet the following communication requirements for an autonomous grain cart: (i) capability for real-time transmit of pose, velocity and fill level, (ii) low energy consumption, (iii) kilometer-level range to cover larger fields, and (iv) inexpensive and simple networking configuration.

3) Control Technique: Sensing and V2V communication provide sufficient information for the planner to generate reference motions, tracking which the controller can calculate the throttle, brake, and steering requirements to maneuver the grain cart. To solve this control problem, Proportional, Integral and Derivative (PID) control, the most extensively used feedback control technique, can be adopted. PID has played a dominant role in process control because it is simple, efficient, and generally applicable to most control systems. It has been proven that PID has the potential to provide optimal control solutions for vehicle motion control, which is characterized by nonlinear dynamics, unmeasured disturbances, noise, measurement delays and lags [21], [22]. The controller design primarily consists of the process of tuning the PID gains, which is omitted herein in favor of space.

4) Actuation Plan: Most traditional drive trains are mechanical and provide direct, physical control over the speed or direction, which is not always practical to deliver actuation functions in autonomous driving. In contrast, drive-by-wire powertrains can support the automation of farming vehicles as they are primarily composed of servomotors or electromechanical actuators that are directly controlled through electric wires instead of mechanical connections. Drive-by-wire functionalities (e.g., steer, throttle, and brake) are already available from major farm equipment manufacturers like John Deere, CNH, AGCO, CLASS and Kubota [23].

B. Planning Algorithm

1) Theoretical Basis and Rationale: Motion (path) planning has been a popular subject of study in mobile robotics, where different planning algorithms have been employed. For example, resistance network for path planning plus MPC for local motion planning [24], dangerous-potential-field-based path planning for collision avoidance [25], probabilistic occupancy grid for motion planning considering localization uncertainty, ego-vehicle constrains and obstacles [26], dynamic programming for path pre-selection and obstacle-avoiding re-planning [27], nonlinear programming for motion primitive optimization plus A* algorithm for path search plus gradient-based path smoothing [28], genetic algorithm for global path planning plus local rolling optimization in a UAV&UGV cooperative system [29], and particle swarm optimization for a search-and-track mission [30]. Thorough reviews and comparisons of the

above and other commonly used techniques (e.g., Artificial Potential Field, sampling-based methods, Fuzzy Logic Control, Neural Networks, etc) have been carried out by a number of studies [31]–[35], which have demonstrated that each technique has its own advantages as well as limitations. In this study, two classic algorithms, Artificial Potential Field (APF) and Fuzzy Logic Control (FLC) were selected because when integrated in a novel way, they could form a sophisticated yet intuitive planner for autonomous grain carts. The rationale is as follows.

APF refers to the potential field "constructed" by the potential functions artificially assigned to the goal and the obstacles in the navigation task. The potential functions are specifically designed such that taking the gradient of them generates attractive forces towards the goal and repulsive forces from the obstacles. The farther from the goal, the greater the attractive forces; the closer to the obstacles, the greater the repulsive forces. The vehicle is assumed to navigate under the influence of the resultant forces, which will lead the vehicle to the goal while keeping it away from the obstacles. Compared with other algorithms, APF is known for its mathematical elegance and simplicity as well as its computational efficiency, which makes it suitable for online feedback planning and control. However, this technique suffers from a major drawback that often compromises the plan's rationality and efficiency; when there is a cancellation of attractive and repulsive forces, the vehicle may become stagnant at or wander around points other than the goal, a situation known as being trapped in local minima. Due to the force cancellation or contradiction, the robot may also experience oscillations in long narrow corridors and not be able to pass between closely spaced obstacles [36].

To fully exploit the advantages of APF and overcome its limitations, we proposed the following improvement strategy. (i) To reduce the probability for local minima traps, set the influence range of the repulsive forces from the obstacles to be small so that they are only effective when the grain cart travels dangerously close to obstacles; when the grain cart is safely away from the obstacles, another algorithm should be able to generate rational and efficient motion plans that can lead the grain cart to go around obstacles and avoid potential local minima in advance. (ii) Noting that a human operator can expertly navigate the grain cart to commute between the semi-trailer and the combine while avoiding different types of obstacles, their operational knowledge, experience, and intuition can be leveraged to perform efficient motion planning.

Fuzzy Logic (FL) resembles the human decision-making methodology and compared with other algorithms, FL is simple, efficient, and robust in spite of uncertainty and imprecise information. Any event, process, or function that evolves continuously cannot always be characterized by either true or false; therefore, compared with binary logic that only looks at absolute truth (1) or falseness (0), FL that deals with membership values in the range of [0, 1] (closer to 0: higher tendency towards falseness; closer to 1: higher tendency towards truth) can often be more practical in solving real-world problems. FL first breaks down a problem into a number of simple tasks, then addresses each task, applying the associated set of fuzzy rules developed based on human experts' heuristic knowledge, experience, or intuition, which normally take the form of IF...THEN... When an input does not precisely correspond to any predefined rule, partial matching of the input is used to interpolate an answer. Facing the challenge that navigation in dynamic agricultural environments requires fast reactions to uncertainties while the behaviors of agricultural vehicles are often too complex to be modeled accurately, Fuzzy Logic Control (FLC) can directly leverage knowledge and experience and intuition as well as the imprecise reasoning and decision-making mechanism of human operators to provide planning solutions quite efficiently. FLC is thus a good choice for overcoming the deficiencies of APF. One may argue that FLC is not as precise as optimization-based algorithms and can only provide "good enough" solutions. In fact, achieving mathematically optimal solutions was not the goal in this study. Unlike on-road vehicles that are normally required to accurately follow specific trajectories, grain carts work in wide open crop fields, where meter-level errors are acceptable. Besides, modeling the nonlinear behaviour of the grain cart over uneven and slippery terrain is extremely challenging, thus implementing an "optimal" plan is not always practical. In terms of safety concerns, APF serves as a safety guard by enabling prompt collision avoidance with close obstacles.

2) APF Construction: The scope of the study was limited to a plain field (i.e., no significant slopes or curves) that can be represented by a 2D configuration space (i.e., C-space, the set of all positions the vehicle may attain). The host-vehicle's position is symbolized by $q = (x, y)$. Correspondingly, the attractive and repulsive potentials at q as well as their summation are $U_{att}(q)$, $U_{rep}(q)$, and $U(q)$, respectively. With $U(q)$ being differentiable for every q in the C-space, the resultant artificial force is

$$\overrightarrow{F}(q) = -\nabla U(q) = -\nabla U_{att}(q) - \nabla U_{rep}(q), \tag{1}$$

where $\nabla U(q)$ denotes the gradient of U at q, namely a vector pointing at the direction of fastest change of U at (x, y). In a 2D C-space, the gradient can be calculated as

$$\nabla U(q) = \begin{bmatrix} \frac{\partial U}{\partial x} \\ \frac{\partial U}{\partial y} \end{bmatrix}. \tag{2}$$

Looking at the attractive potential first, the farther away the vehicle from the goal, the greater the $U_{att}(q)$. Therefore, a possible form of the attractive potential is

$$U_{att}(q) = \frac{1}{2}\xi\rho^2(q_{goal}), \tag{3}$$

where ξ is a constant scaling factor (that can be determined experimentally) and $\rho(q_{goal})$ is the distance between the vehicle and the goal. In a general C-space which is not necessarily 2D,

$$\rho(q_{goal}) = \|q - q_{goal}\| = \sqrt{\sum (x_i - x_{gi})^2}, \tag{4}$$

where $q = (x_1, x_2, \ldots, x_n)$ and $q_{goal} = (x_{g1}, x_{g2}, \ldots, x_{gn})$ are the coordinates of the host-vehicle and the goal, respectively. Therefore, the attractive force can be derived as follows.

$$\begin{aligned}\overrightarrow{F_{att}}(q) &= -\nabla U_{att}(q) \\ &= -\nabla \frac{1}{2}\xi\rho^2(q_{goal}) \\ &= -\xi\rho(q_{goal})\nabla\rho(q_{goal}),\end{aligned} \tag{5}$$

where

$$\begin{aligned}\nabla\rho(q_{goal}) &= \nabla\sqrt{\sum(x_i - x_{gi})^2} \\ &= \frac{\sum(x_i - x_{gi})}{\sqrt{\sum(x_i - x_{gi})^2}} \\ &= \frac{q - q_{goal}}{\|q - q_{goal}\|}.\end{aligned} \tag{6}$$

Substituting Eqns (4) and (6) into Eqn (5), we obtain the attractive force as a vector whose direction is from q to q_{goal}, attracting the vehicle to the goal:

$$\overrightarrow{F_{att}}(q) = -\xi\|q - q_{goal}\|\frac{q - q_{goal}}{\|q - q_{goal}\|} = \xi(q_{goal} - q). \tag{7}$$

Eqn (7) indicates that the magnitude of the attractive force is proportional to the distance between the goal and the vehicle; when the vehicle approaches the goal, $\overrightarrow{F_{att}}(q)$ converges to zero, which is reasonable, yet when the vehicle moves away from the goal, $\overrightarrow{F_{att}}(q)$ grows without a bound, which could be unstable. To keep $\overrightarrow{F_{att}}(q)$ bounded, a hybrid concept can be adopted that replaces $\frac{1}{2}\xi\rho^2(q_{goal})$ with $\xi d\rho(q_{goal})$ for $U_{att}(q)$ when the distance between the vehicle and the goal is greater than the predefined threshold d, meaning

$$\overrightarrow{F_{att}}(q) = -\nabla U_{att}(q) = -\xi d\frac{q - q_{goal}}{\|q - q_{goal}\|}. \tag{8}$$

Thus the complete representations of the attractive potential and force are as follows.

$$U_{att}(q) = \begin{cases}\frac{1}{2}\xi\rho^2(q_{goal}) & \text{if } \rho(q_{goal}) \le d \\ d\xi\rho(q_{goal}) & \text{if } \rho(q_{goal}) > d\end{cases}, \tag{9}$$

$$\overrightarrow{F_{att}}(q) = \begin{cases}-\xi\|q - q_{goal}\|\frac{q-q_{goal}}{\|q-q_{goal}\|} & \text{if } \|q - q_{goal}\| \le d \\ -\xi d\frac{q-q_{goal}}{\|q-q_{goal}\|} & \text{if } \|q - q_{goal}\| > d\end{cases}. \tag{10}$$

Correlating Eqn (10) with the motion planning task for autonomous grain carts, q represents the current position of the grain cart, q_{goal} represents the position of current goal, which can be a point by the left side of the combine or the semi-trailer, or simply a standby point. Determination of this target position is described in *B.5) Task Scheduling*. Determination of d depends on the scale of the crop field relative to the grain cart; large fields may allow greater d while compact fields require smaller d. In contrast to the attractive potential, the repulsive potentials increase as the vehicle moves closer to the obstacles. Consequently, a repulsive potential can be simply structured as

$$U_{rep}(q) = \begin{cases}\frac{1}{2}\eta\left(\frac{1}{\rho(q_{obs})} - \frac{1}{\rho_0}\right)^2 & \text{if } \rho(q_{obs}) \le \rho_0 \\ 0 & \text{if } \rho(q_{obs}) > \rho_0\end{cases}, \tag{11}$$

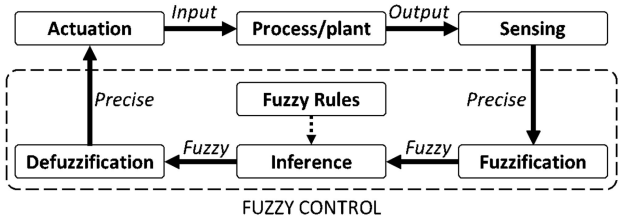

Fig. 2. A typical closed-loop FLC process.

where η is a scaling factor, $\rho(q_{obs})$ is the distance between the vehicle and the detected obstacle, and ρ_0 is a positive constant standing for the obstacles' influence range. Similar to the attractive potential, the repulsive potentials are formed in a hybrid fashion so that the influences of the distant obstacles are neglected. Taking gradient of $U_{rep}(q)$ when it is not 0, the repulsive force is obtained as below.

$$\begin{aligned}\overrightarrow{F_{rep}}(q) &= -\nabla U_{rep}(q) \\ &= -\nabla\frac{1}{2}\eta\left(\frac{1}{\rho(q_{obs})} - \frac{1}{\rho_0}\right)^2 \\ &= \eta\left(\frac{1}{\rho(q_{obs})} - \frac{1}{\rho_0}\right)\frac{1}{\rho^2(q_{obs})}\nabla\rho(q_{obs}).\end{aligned} \tag{12}$$

By analogy with the derivation of $\nabla\rho(q_{goal})$ in Eqn (6),

$$\nabla\rho(q_{obs}) = \frac{q - q_{obs}}{\|q - q_{obs}\|}, \tag{13}$$

where q_{obs} is the position of the obstacle. Thus, $\nabla\rho(q_{obs})$ is a unit vector directed from q_{obs} to q, "pushing" the vehicle away from the obstacles. The complete representation of the repulsive force is

$$\overrightarrow{F_{rep}}(q) = \begin{cases}\left(\frac{1}{\rho(q_{obs})} - \frac{1}{\rho_0}\right)\frac{\eta(q-q_{obs})}{\rho^2(q_{obs})\|q-q_{obs}\|} & \text{if } \rho(q_{obs}) \le \rho_0 \\ 0 & \text{if } \rho(q_{obs}) > \rho_0\end{cases} \tag{14}$$

In this study, $\rho(q_{obs})$ represents the distance between the grain cart and the closest obstacle point detected by the sensor; ρ_0 should be properly small (based on specification of safety distance and dimensions of the vehicles) for the crops, combine and semi-trailer as the grain cart sometimes needs to operate close to them; meanwhile, ρ_0 can be large for other random static and dynamic obstacles that the grain cart should stay safely away from.

Summing the attractive and repulsive forces, the resultant artificial potential force is converted to motion planning via a widely used conversion technique, force to velocity [37], where the magnitude and direction of the resultant force, respectively, determine the desired linear velocity and heading.

3) FLC Formulation: Fig. 2 illustrates how a typical closed-loop FLC process is formulated. In response to actuation, the process to be controlled generates the output, which is sampled and measured by the sensors. This measurement is usually a precise quantity and is first "fuzzified" into a fuzzy quantity that, with different degrees of membership, belongs to a number of fuzzy sets. Following the predefined linguistic fuzzy rules,

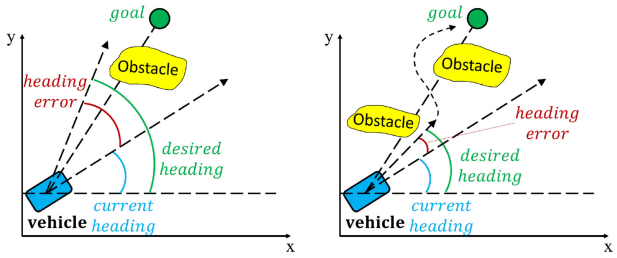

Fig. 3. Heading errors with single and multiple obstacles.

the fuzzy controller then makes decisions based on the fuzzified measurement. The fuzzy decision is also in the form of a number of fuzzy sets (with different degrees of membership) and is eventually converted into a precise quantity with defuzzification methods. Finally, the defuzzified control command is carried out by the actuation system to regulate the behavior of the process, starting a new control cycle. In this study, the sensors take measurements of the linear velocity and heading. The FLC part of the proposed planner uses the measurements to calculate the desired steering angle as the planner output, based on which the controller will determine control commands. Last, the actuators will carry out the control to regulate the behavior of the grain cart.

Fuzzy rules are the core of FLC and leverage human operators' knowledge, experience, and intuition. In this study, it makes intuitive sense that the grain cart steers fast to avoid the obstacles efficiently; yet, it should not steer fast so that the stability of the tractor (as well as the comfort and safety of the human supervisor in the cab, if any) can be ensured. Considering the complexity and nonlinearity of the grain cart's behavior traveling in the field over unpredictably uneven and slippery terrain, finding the optimal balance between steering efficiency and stability (as well as safety and comfort) is challenging. However, from the human operator's point of view, the solution to this planning problem is simple and clear; the larger the difference between the desired and current headings (i.e., heading error), the greater the steering angle; meanwhile, the higher the (current, not desired) linear velocity, the smaller the steering angle.

Compared with the measurement of current linear velocity, the determination of heading error is complex (Fig. 3); when a single obstacle blocks the straight path to the goal, the vehicle should go around it from the closer side (i.e., the side the goal is closer to); when multiple obstacles block the straight path to the goal, the vehicle should deal with them one by one (starting from the closest) from the closer side, exploring the openings between the obstacles.

Following the FLC process in Fig. 2, the precise measurements of the current linear velocity and heading error are first fuzzified into fuzzy quantities. While linear velocity can be described as Slow, Normal and Fast, heading error can be characterized as Far Right, Right, Front, Left, and Far Left, which indicate the direction of the desired heading relative to the current heading (left being positive, right being negative). The membership functions associated with these two measurement quantities are shown in Fig. 4. Note that different operators with different driving habits and experience have different

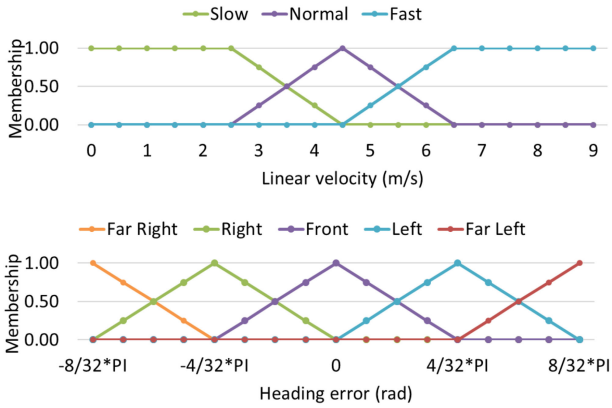

Fig. 4. Membership functions of FLC inputs.

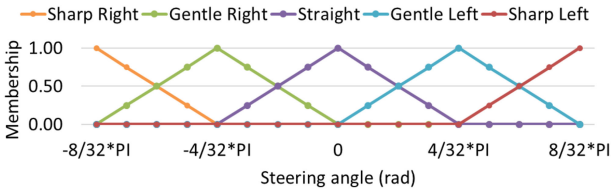

Fig. 5. Membership functions of FLC output.

TABLE I
FUZZY RULES FOR STEERING PLANNING

	Far Right	Right	Front	Left	Far Left
Slow	Sharp Right	Sharp Right	Straight	Sharp Left	Sharp Left
Normal	Sharp Right	Gentle Right	Straight	Gentle Left	Sharp Left
Fast	Gentle Right	Gentle Right	Straight	Gentle Left	Gentle Left

judgements on the membership values. The values in this study were determined based on (i) authors' driving experience and observation of real harvest operations, (ii) discussion from online forums on crop harvesting, and (iii) the scaling of the simulation tests. Before formulating the fuzzy rules, fuzzy sets and membership functions of the fuzzy decision need to be defined, wherein the desired steering angle is expressed in terms of Sharp Right, Gentle Right, Straight, Gentle Left, and Sharp Left, whose membership functions are shown in Fig. 5. Given the fuzzy sets of both the input (heading error and linear velocity) and output (desired steering angle) of the fuzzy controller, the linguistic fuzzy rules are tabulated in Table I. Finally, the fuzzy steering decision can be defuzzified into a precise steering angle in radians and input to the controller. While various defuzzification techniques are available, weighted average method is adopted herein for its computational simplicity [38].

4) Integration Mechanism: As described above, APF is based on elegant mathematical concepts and operations that support fast planning in real-time applications; yet simply following the equations could generate irrational or inefficient motion plans. Meanwhile, FLC leverages human intelligence

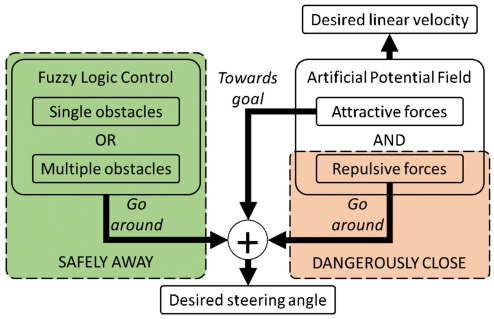

Fig. 6. Integration mechanism of APF and FLC.

that can take into account the rationality and efficiency of the plan, complementing APF. That being said, some cases are so intractable that formulating fuzzy rules becomes complex and impractical. For example, dynamic obstacles may move around randomly, interfering with the grain cart's motion, in which case APF's attractive and repulsive forces can provide more direct guidance to the grain cart. Integrating APF and FLC is a hybrid approach that is expected to exploit the merits of both techniques while overcoming their limitations. Fig 6. illustrates how APF and FLC are integrated. The attractive forces of APF always decide the heading towards the goal; when the grain cart is safely away from the obstacles, FLC applies simple and effective human-intelligence-based rules to generate collision-free motion plans that account for the GLOBAL efficiency of the motion; when the grain cart gets dangerously close to the obstacles that FLC has not handled (e.g., closely surrounding static and/or fast approaching dynamic obstacles), the repulsive forces of APF enable prompt avoidance of these LOCAL obstacles. As discussed in II-B2, in parallel with the planning for steering angle, APF is also responsible for determining the linear velocity. One may argue that properly adjusting the influence ranges of the goal and obstacles can upgrade the APF algorithm, but developing explicit rules to adapt the APF to the agricultural environment that is largely unconstructed and unpredictable can be a great challenge.

5) Task Scheduling: As previously described, the grain cart should ideally meet the combine exactly when the combine reaches its capacity, a difficult and often impractical challenge. Therefore, to guarantee that harvest is not interrupted, the grain cart typically arrives early and follows the combine before unloading starts. With the goal of reducing this non-productive following time, a special task scheduling strategy was proposed: after the grain cart transfers the grain to the semi-trailer, it should neither stay still waiting for the combine's unloading request nor go and follow the combine until unloading starts; instead, the grain cart should drive to the boundary of the working area where the combine is harvesting crops, then stand by in a position from which a clear path to the combine is available. "Clear" simply implies that between the grain cart and the combine, there are no blocking obstacles (not even unharvested crop rows), allowing the grain cart to approach the combine via a straight route (additional maneuvers might be needed for heading alignment). Thus a motion plan that meets the temporal requirement can be easily computed based on the relative poses and velocities

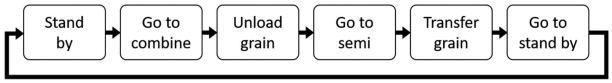

Fig. 7. Work cycle of an autonomous grain cart.

of the two vehicles as well as the fill level of the combine transmitted to the cart via wireless communication. The work cycle of an autonomous grain cart is illustrated in Fig. 7. It can be seen that, in addition to unloading grain from the combine, logistical tasks for grain carts in harvest operations include stand by when the combine is harvesting, navigate through the field to meet the combine when unloading is needed, navigate to the semi-trailer, transfer the grain to the semi-trailer and return to the standby point. To sequence and schedule these tasks, the following triggers are specified.

Go to combine: **IF** standing by **AND** combine full by arrival of grain cart **THEN** go to combine

Unload combine: **IF** close to combine **AND** aligned with combine **THEN** drive alongside combine in sync (when to start and finish unloading is determined by combine)

Go to semi: **IF** combine empty **OR** grain cart full **THEN** go to semi

Transfer grain to semi: **IF** going to semi **AND** close to semi **AND** aligned with semi **THEN** transfer grain to semi

Go to standby point: **IF** transferring grain **AND** grain cart empty **THEN** go to standby point

Stand by: **IF** going to standby point **AND** close to standby point **AND** facing specified direction **THEN** stand by

C. Simulation Tests

1) Experimental Setup: A set of simulation tests were conducted to investigate the effectiveness, robustness, efficiency, and computational expense of the proposed motion planning algorithm. MatLab Simulink R2019a was employed as the simulation platform. To imitate an actual crop harvest, a 2D virtual harvest operation was modeled, executed (at 50 Hz) and plotted (Fig. 8): a semi-trailer (in pink) waited nearby, a trapezoidal crop field (in orange) was harvested row by row by a combine (in green), a grain cart (in blue) unloaded and transferred the grain; real-time fill levels of the combine and grain cart were shown on the bottom left of the plot. The simulated harvest was downscaled from real harvests in terms of crop row lengths and combine capacity. The goal was to use minimal time and space to showcase the effectiveness of the proposed planning algorithm in various scenarios that could be encountered by grain carts in harvest operations.

2) Field Data: A set of yield monitor data from a corn field in Minnesota were incorporated into the simulation tests. Specifically, the crop flow and combine speed collected by a combine throughout a harvest operation were processed and utilized to validate the specification of the fill rate and speed of the simulated combine. Because the simulation tests were downscaled from real harvest operations, instead of the actual mean and standard deviation, the coefficients of variation of the crop flow and combine speed were employed, which reflected the

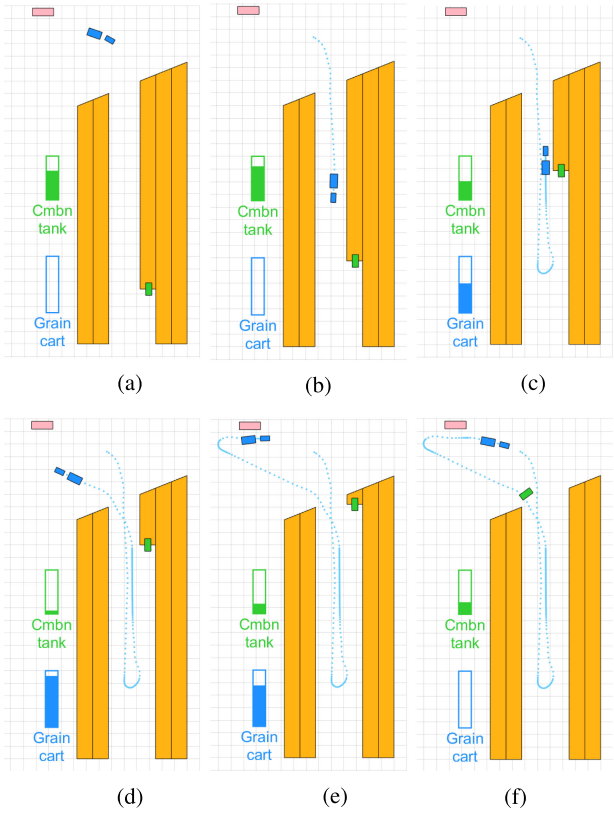

Fig. 8. Example of a work cycle in simple harvesting. (a) Standby. (b) To combine. (c) Unload. (d) To semi. (e) Transfer. (f) To standby.

extent of variabilities in relation to the means. The coefficients of variation of the crop flow and combine speed were 5.61% and 3.24%, respectively.

3) Test Design. Simple Harvesting: In this test, unharvested crop rows were the only obstacles, and the grain cart was expected to follow the generated motion plans and autonomously accomplish all the logistical tasks.

Static Obstacles: Six square static obstacles were placed between the crop rows and the semi-trailer. The grain cart was expected to navigate around them and accomplish the logistical tasks. For a more rigorous test of robustness, the configuration of the obstacles varied every work cycle.

Dynamic Obstacles: This test involved the wandering motion of two rectangular obstacles (one revolving, one back and forth) between the crop rows and the semi-trailer, intermittently impeding the grain cart. The grain cart was expected to anticipate all potential collisions, avoid them and eventually find its way to the goal.

Same Tests with APF: Another set of three simulation tests like those above were conducted with a simple APF planner guiding the grain cart. Data from both sets of tests were collected and compared.

4) Data Collection and Results Analysis. Effectiveness and Robustness: The first aspect considered was whether the proposed planner was effective in directing the grain cart to autonomously accomplish the logistical tasks. Task accomplishment in simple and complex harvest operations (involving static and dynamic obstacles) would verify the effectiveness and robustness of the proposed motion planning algorithm. This analysis provided a qualitative result. As mentioned previously, the focus of the proposed task scheduling strategy is on reducing the non-productive following time, which is measured from the moment the grain cart reaches the left side of the combine until the unloading starts. This analysis provided a quantitative result. No comparison between the proposed planner and simple APF planner was conducted for meeting timing because the task scheduling was not involved in the simple APF algorithm at all. In addition, when random static or dynamic obstacles were present, they interfered with the grain cart in unpredictable ways, hindering it from performing the tasks on time. Therefore, meeting timing was not considered for these cases.

Efficiency: The evaluation was based on the comparison between the proposed planner and the simple APF planner in the length and smoothness of the grain cart's trajectory. In simple harvesting, the comparison ran through the entire harvest operation. In the harvest cases involving static and dynamic obstacles, the comparison was focused on how differently the two planners dealt with the obstacles. Therefore, only when the grain cart was out of the crop rows, either going to the semi-trailer or returning to the standby point, the trajectories were measured and compared. To measure the smoothness of the trajectory, the formula of $\kappa' = \frac{1}{n}\sum_{i=2}^{n}\alpha_i^2$ was used, where κ' represents the smoothness, α_i is the angle between two consecutive segments of the trajectory, and n is the total number of segments the trajectory consists of. Assuming the mean of α_i is zero, κ' is the variance of α_i with a unit of rad^2. Measurements of both length and smoothness provided quantitative results.

Computational Expense: The CPU time the motion planning computation consumed in each simulation step was additional important data to collect, which also provided a quantitative result. Computational efficiency has been discussed in many studies [32], [34], [35] as a key advantage of APF over other techniques, demonstrating that APF is suitable for real-time applications. Since the proposed motion planning algorithm incorporated FLC into APF, it was expected to be more computationally expensive than the simple APF.

D. Mobile Robot Tests

1) Experimental Setup: A set of mobile robot tests were conducted to verify the effectiveness and practicality of the proposed navigation solution. A Jackal (by Clearpath Robotics, Inc.) represented the grain cart and a TerraSentia (by EarthSense, Inc.) represented the combine. The TerraSentia was remotely controlled by a human with the paired tablet computer. For simplicity, a cardboard box was employed to represent the semi-trailer. For local perception, a scanning laser rangefinder (Model UTM-30LX by Hokuyo) was employed and mounted on top of the Jackal. For localization of the Jackal and TerraSentia in the indoor experimental environment, two identical tracking cameras (Model RealSense T265 by Intel Corp.) were employed (instead of RTK-GPS which is typically for outdoor uses). The tracking cameras also featured onboard IMUs, which were used to measure the linear velocities and headings of the Jackal and TerraSentia. A mini PC (Model NUC6i5SYK by Intel Corp.)

was employed to run the sensors on the Jackal. A gaming laptop (Model G5 by Dell Corp.) was mounted on top of the TerraSentia to run the tracking camera as well as interact with the mini PC remotely. A laptop (Model ThinkPad T580 by Lenovo Corp.) served as the computation hub, executing the core planning and control algorithms. The laptop communicated wirelessly with the computer onboard the Jackal, the Intel mini PC on the Jackal and the Dell laptop on the TerraSentia. TAMULink, Texas A&M University's campus wireless network was adopted for the communication between the computing devices and a Robot Operating System (ROS) network was built for transmitting the sensing and control messages. Cardboard sheets were employed to represent the crop rows. The cardboard sheets were placed vertically on the ground with certain angles relative to each other. Slightly folded on the side and attached to the ground with duct tape, the cardboard sheets stayed upright by themselves, and they were easily run over by the TerraSentia robot. When standing upright, the cardboard sheets resembled unharvested crop rows that could potentially block the Jackal; when run over, the cardboard sheets resembled harvested areas that could be traversed by the Jackal.

2) Test Design: Two very common cases of crop harvest were tested. With the grain cart (Jackal) and the combine (TerraSentia) meeting for unloading, they traveled (i) in the same direction and (ii) opposite directions. When facing the same direction, the grain cart could directly approach the combine. When facing opposite directions, the grain cart needed to make a U-turn to align its heading with that of the combine before unloading started. Beginning at the standby point, the grain cart needed to accomplish all the logistical tasks described previously (Fig. 7). Note that the comparison between the APF and APF+FLC planners was not conducted, primarily because the obstacle avoidance tasks herein were relatively simple and would not help showcase the advantage of the proposed algorithm.

3) Results Analysis: The primary consideration was whether the proposed navigation solution was effective and practical, which provided a qualitative result. If the grain cart could autonomously accomplish all the logistical tasks, it would be reasonable to declare that the proposed navigation solution, featuring 2D-lidar-based local perception, IMU-based vehicle states measurement, Wi-Fi-supported V2V communication, and drive-by-wire actuation, was effective and practical in implementing the developed motion planning algorithm.

III. Results and Conclusions

A. Simulation Tests

1) Simple Harvesting. Effectiveness: When no obstacles other than unharvested crop rows were present, both the APF+FLC and APF planners were effective in directing the grain cart in the crop field to accomplish all the logistical tasks without any collisions. Fig. 8 exemplifies a work cycle of the autonomous grain cart. For the six unloading operations that took place during the entire harvest, the grain cart spent an average of only 5.38 s following the combine before unloading started. This non-productive following time was less than 0.6% of the total time of the simulated harvest operation, which was 15 minutes.

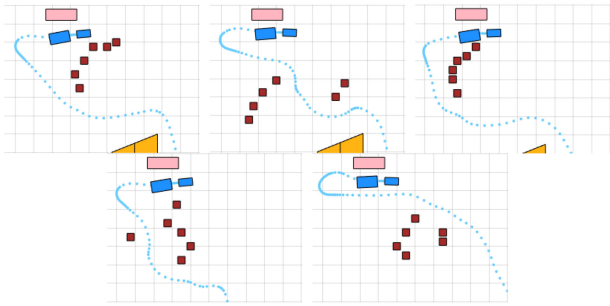

Fig. 9. APF+FLC planner dealt with static obstacles.

Therefore, the effectiveness of the proposed motion planning algorithm and the task scheduling strategy was verified.

Efficiency: The two planners differed from each other in two scenarios: (i) each time the grain cart left the combine for the semi-trailer, the APF planner tended to drive the grain cart unnecessarily close to the crop rows while the APF+FLC planner, leveraging human-like intelligence, kept the grain cart safely away from the rows; (ii) due to its inherent limitations, the APF planner made the grain cart oscillate when it was traveling between the crop rows, while the APF+FLC had no such issue. Therefore, in terms of rationality of the motion plans, the APF+FLC planner outperformed the APF planner. In terms of the trajectory length and smoothness, the APF+FLC trajectory was slightly smoother (0.00 062 rad^2) while slightly longer (1590.89 m) than the simple APF trajectory (0.00 063 rad^2 for smoothness and 1583.37 m for length). These results imply that, overall, the two planners generated similar motion plans. Two major reasons for the lack of difference in performance between the planners in this test were (i) the obstacle avoidance task was relatively simple when unharvested crop rows were the only obstacles, and (ii) the standby point was deliberately selected such that a straight route to the unloading location was always available, further simplifying the obstacle avoidance task.

Computational Expense: Upgraded from APF, the proposed APF+FLC planner consumed an average CPU time of 0.74 ms in each computation step. Although this computation expense was over two times greater than that of the simple APF planner, which was 0.28 ms, the APF+FLC computations were still very fast. Note that employed for running the simulations was an ordinary CPU (Intel Core i7-8650 U CPU @ 1.90 GHz), thus it is reasonable to declare that the proposed algorithm is sufficiently expeditious for real-time motion planning.

2) Static Obstacles. Effectiveness and Robustness: Both the APF+FLC and APF planners were similarly able to direct the autonomous grain cart to accomplish the logistical tasks, verifying the effectiveness and robustness of the proposed motion planning algorithm and the task scheduling strategy.

Efficiency: A major difference between the efficiencies of the motions generated by the two planners was observed. Fig. 9 and Fig. 10, respectively, show how the APF+FLC and APF planners handled five sets of static obstacles that blocked the straight route when the grain cart was going to the semi-trailer. Taking early actions to smoothly go around the obstacles from the side closer to the goal enabled the APF+FLC planner to deal with the static

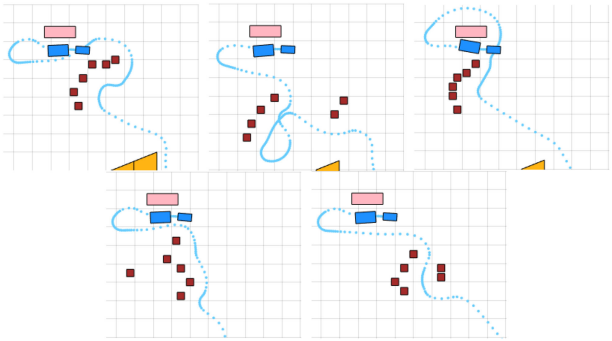

Fig. 10. APF planner dealt with static obstacles.

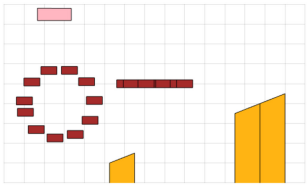

Fig. 11. Moving pattern of two dynamic obstacles: one revolved, one moved back and forth.

obstacles more rationally and efficiently, with a trajectory length of 436.74 m and smoothness of 0.0014 rad^2. In contrast, without a global view, the APF planner steered the grain cart only to avoid imminent collisions with local obstacles, resulting in a trajectory with length of 553.13 m and smoothness of 0.0016 rad^2. Thus, the APF+FLC trajectory was 21.04% shorter and 12.50% smoother than that of the simple APF planner.

Computational Expense: Although the static obstacles made the environmental condition more complex, this fact did not increase the computational expense of the proposed planner as well as the simple APF planner. The average CPU times consumed in each computation step were basically the same as those in the previous test.

3) Dynamic Obstacles. Effectiveness and Robustness: The dynamic obstacles constantly changed the environment between the crop rows and the semi-trailer (Fig. 11). When the grain cart approached this type of obstacles, the APF+FLC planner first made use of FLC and attempted to drive the grain cart around the obstacles based on their configuration, and it updated the motion plan accordingly in each computation step. When dangerously close to the obstacles, the planner relied on APF to promptly avoid potential collisions. As shown in Fig. 12, in some cases the grain cart went around the obstacles from the side, while in other cases the grain cart navigated through the obstacle zones when the wide gap between them provided more efficient routes. Because of the dynamic nature of this test, the "go-around" plans generated by the FLC part of the planner were often overruled as the obstacles typically moved very close to the grain cart, making APF dominate the planning. Both the APF and APF+FLC planners successfully handled the dynamic obstacles and accomplished the logistical tasks, further verifying their effectiveness and robustness.

Efficiency: The APF planner was effective and prompt in avoiding collisions with dynamic obstacles but ended up with a

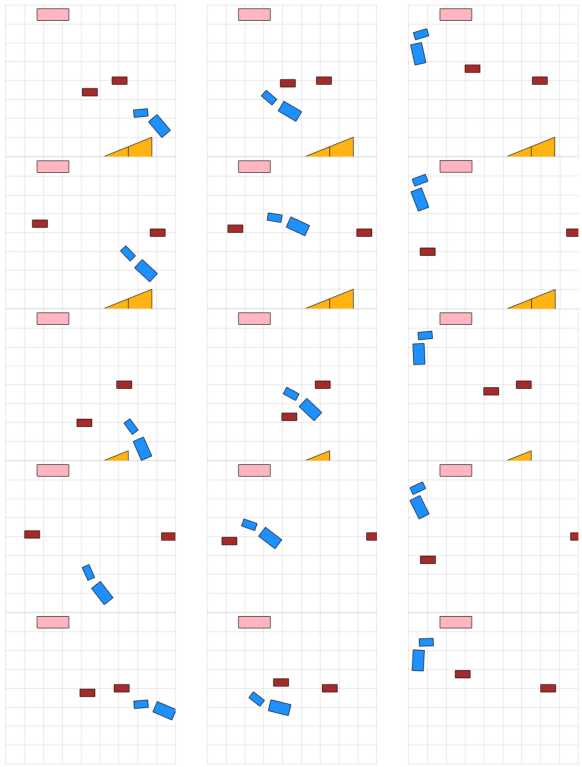

Fig. 12. APF+FLC planner handled dynamic obstacles; each row for each work cycle; sequential motion from left to right.

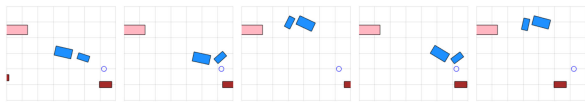

Fig. 13. APF planner had trouble approaching standby point (blue circle); sequential motion from left to right.

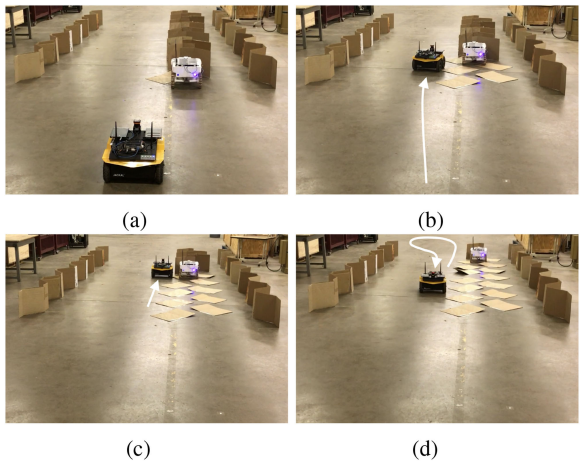

Fig. 14. Grain cart accomplished logistical tasks when combine had same facing. (a) Standby. (b) To combine. (c) Unload. (d) To semi.

trajectory that was 831.18 m in length and 0.0012 rad^2 in smoothness, compared with the APF+FLC trajectory that was 18.76% shorter (675.27 m) and 16.67% smoother (0.0010 rad^2). The primary reason for these differences was that, with the APF planner, the grain cart occasionally got trapped in a local minimum. In these instances, when the dynamic obstacle was wandering close

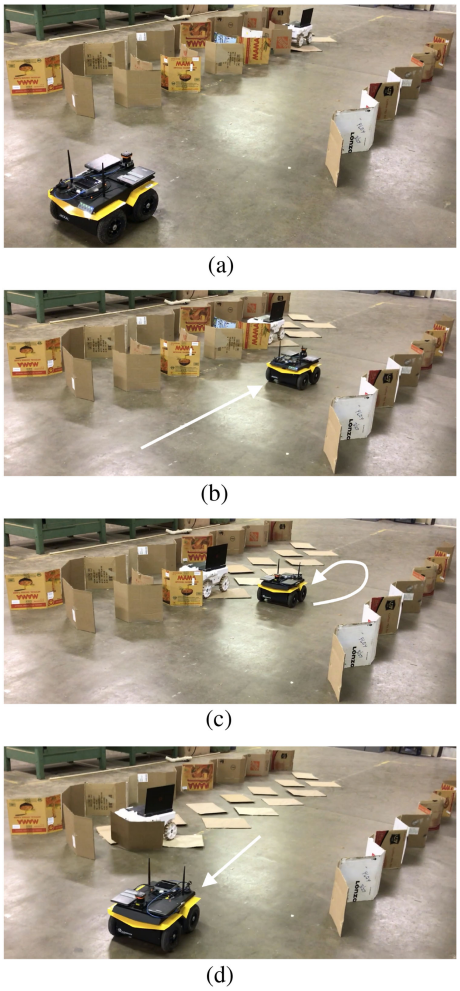

Fig. 15. Grain cart accomplished logistical tasks when combine had opposite facing. (a) Stand by. (b) To combine. (c) Unload. (d) To semi.

to the standby point although not really blocking the grain cart, its repulsive forces hindered the grain cart (which just finished transferring the grain to the semi-trailer) from approaching the standby point in the specified heading. Therefore, the grain cart had to make U-turns to adjust its pose, only to fail again until the dynamic obstacle moved away (Fig. 13). In contrast, the APF+FLC planner had no such issue since it has the intelligence to ignore the dynamic obstacle, which actually never blocked the way to the standby point. Compared with the APF planner, the APF+FLC planner exhibited higher efficiency handling dynamic obstacles in this study.

Computational Expense: Dealing with the dynamic obstacles did not add significant extra calculation requirements to the CPU, leaving the computational expenses of both planners similar to those in the previous tests.

B. Mobile Robot Tests

In both test cases – when the grain cart (Jackal) and combine (TerraSentia) faced the same direction or opposite directions when meeting for unloading – the proposed navigation solution, implementing the APF+FLC planner along with the task scheduling strategy, was able to direct the autonomous grain cart to accomplish all the logistical tasks. Illustrated in Fig. 14 and Fig. 15, where the grain cart and combine faced the same direction or opposite directions, respectively, the autonomous grain cart stood by, went to the combine, unloaded the grain, and went to the semi-trailer (grain transfer and return to standby point were omitted in favor of space). Therefore, the effectiveness and practicality of the proposed navigation solution were verified.

C. Conclusion

A motion planning algorithm with an associated high-level navigation solution was proposed for autonomous grain carts. The algorithm exploits the merits of APF and FLC by integrating them in a novel fashion so that they complement each other to form a more intelligent planning mechanism. The navigation solution provided the technology platform for implementing the proposed planner, covering sensing, communication, control and actuation. The simulation tests demonstrated that, with the associated task scheduling strategy, the proposed planner can generate collision-free motion plans in real time to guide the autonomous grain cart to accomplish the assigned logistical tasks in the harvest operations, guarantee the continuity of harvesting with negligible non-productive following time as well as handle static and dynamic obstacles with motions more efficient than those of the simple APF planner. Therefore, the effectiveness, robustness, efficiency and computational ease of the proposed planning algorithm have been verified. In the mobile robot tests, the proposed high-level navigation solution implementing the motion planning algorithm successfully directed the grain cart to autonomously navigate between the crop rows to accomplish the logistical tasks in the harvest operations, with the combine traveling in the same and opposite directions. Therefore, the proposed navigation solution has been verified to be effective and practical. Experiments with real grain carts and combines are needed for further verification before the proposed planning algorithm can be applied in actual harvest operations.

REFERENCES

[1] "Economic information bulletin," United States Department of Agriculture, Economic Research Service, doi: 10.22004/ag.econ.281161.
[2] O. Ali, B. Verlinden, and D. Van Oudheusden, "Infield logistics planning for crop-harvesting operations," *Eng. Optim.*, vol. 41, no. 2, pp. 183–197, 2009.
[3] D. Bochtis, S. Vougioukas, C. Tsatsarelis, and Y. Ampatzidis, "Field operation planning for agricultural vehicles: A hierarchical modeling framework," *CIGRE*, Feb. 2007, Paper PM 06 021.
[4] Z. L. Huan, T. Tomohiro, and A. Tofael, "Leader-follower tracking system for agricultural vehicles: Fusion of laser and odometry positioning using extended Kalman filter," *IAES Int. J. Robot. Automat.*, vol. 4, no. 1, pp. 1–18, 2015.
[5] N. Noguchi, J. Will, J. Reid, and Q. Zhang, "Development of a master-slave robot system for farm operations," *Comput. Electron. Agriculture*, vol. 44, no. 1, pp. 1–19, 2004.
[6] L. Zhang, T. Ahamed, Y. Zhang, P. Gao, and T. Takigawa," Vision-based leader vehicle trajectory tracking for multiple agricultural vehicles," *Sensors*, vol. 16, no. 4, pp. 578, 2016.
[7] C. Zhang, N. Noguchi, and L Yang, "Leader-follower system using two robot tractors to improve work efficiency," *Comput. Electron. Agriculture*, vol. 121, pp. 269–281, 2016.
[8] S. G. Vougioukas, "A. distributed control framework for motion coordination of teams of autonomous agricultural vehicles," *Biosyst. Eng.*, vol. 113, no. 3, pp. 284–297, 2012.

[9] O. Ali, B. S. Germain, J. Van Belle, P. Valckenaers, H. Van Brussel, and J. Van Noten, "Multi-agent coordination and control system for multi-vehicle agricultural operations," in *Proc. 9th Int. Conf. Autono. Agents Multiagent Syst.*: *Int. Found. Auton. Agents Multiagent Syst.*, 2010, 1621–1622.
[10] I. A. Hameed, D. Bochtis, and C. A. Sørensen, "An optimized field coverage planning approach for navigation of agricultural robots in fields involving obstacle areas," *Int. J. Adv. Robot. Syst.*, vol. 10, no. 5, pp. 1–9, 2013.
[11] D. Bochtis, C. Sørensen, and S. Vougioukas, "Path planning for in-field navigation-aiding of service units," *Comput. Electron. Agriculture*, vol. 74, no. 1, pp. 80–90, 2010.
[12] M. Elbanhawi and M. Simic, "Randomised kinodynamic motion planning for an autonomous vehicle in semi-structured agricultural areas," *Biosyst. Eng.*, vol. 126, pp. 30–44, 2014.
[13] S. D. Bopardikar, S. L. Smith, and F. Bullo, "On dynamic vehicle routing with time constraints," *IEEE Trans. Robot.*, vol. 30, no. 6, pp. 1524–1532, Dec. 2014.
[14] A. W. Kolen, A. Rinnooy Kan, and H. W. Trienekens, "Vehicle routing with time windows," *Operations Res.*, vol. 35, no. 2, pp. 266–273, 1987.
[15] S. Scheuren, S. Stiene, R. Hartanto, J. Hertzberg, and M. Reinecke, "The problem of spatio-temporally constrained motion planning for cooperative vehicles," in *Proc. 26th Workshop "Planen, Scheduling und Konfigurieren, Entwerfen"(PuK 2011)*, 2011.
[16] B. Åstrand and A.-J Baerveldt, "A vision based row-following system for agricultural field machinery," *Mechatronics*, vol. 15, no. 2, pp. 251–269, 2005.
[17] N. Shalal, T. Low, C. McCarthy, and N. Hancock, "A review of autonomous navigation systems in agricultural environments," presented at the Innovative Agricultural Technologies for a Sustainable Future, Barton, Western Australia, Sep. 22–25, 2013.
[18] H. Mousazadeh, "A technical review on navigation systems of agricultural autonomous off-road vehicles," *J. Terramechanics*, vol. 50, no. 3, pp. 211–232, 2013.
[19] V. Subramanian, T. F. Burks, and A. Arroyo, "Development of machine vision and laser radar based autonomous vehicle guidance systems for citrus grove navigation," *Comput. Electron. Agriculture*, vol. 53, no. 2, pp. 130–143, 2006.
[20] G. Reina, A. Milella, R. Rouveure, M. Nielsen, R. Worst, and M. R. Blas, "Ambient awareness for agricultural robotic vehicles," *Biosyst. Eng.*, vol. 146, pp. 114–132, 2016.
[21] B. Mashadi, M. Mahmoudi-Kaleybar, P. Ahmadizadeh, and A. Oveisi, "A path-following driver/vehicle model with optimized lateral dynamic controller," *Latin Amer. J. Solids Structures*, vol. 11, no. 4, pp. 613–630, 2014.
[22] D. H. Kusuma, M. Ali, and N. Sutantra, "The comparison of optimization for active steering control on vehicle using pid controller based on artificial intelligence techniques," in *Proc. Int. Seminar Appl. Technol. Inf. Commun.*, 2016, pp. 18–22.
[23] C. L. C. Baillie, D. A. C. McCarthy, Z. X. A. Thomasson, and S. Sukkarieh, "Developments in autonomous tractors," 2017. Accessed: Dec. 31, 2019, [Online]. Available: https://grdc.com.au/resources-and-publications/grdc-update-papers/tab-content/grdc-update-papers/2017/07/developments-in-autonomous-tractors
[24] Y. Huang, H. Wang, A. Khajepour, H. Ding, K. Yuan, and Y. Qin, "A. novel local motion planning framework for autonomous vehicles based on resistance network and model predictive control," *IEEE Trans. Veh. Technol.*, vol. 69, no. 1, pp. 55–66, Jan. 2020.
[25] J. Ji, A. Khajepour, W. W. Melek, and Y. Huang, "Path planning and tracking for vehicle collision avoidance based on model predictive control with multiconstraints," *IEEE Trans. Veh. Technol.*, vol. 66, no. 2, pp. 952–964, Feb. 2017.
[26] A. Artuñedo, J. Villagra, J. Godoy, and M. D. Del Castillo, "Motion planning approach considering localization uncertainty," *IEEE Trans. Veh. Technol.*, vol. 69, no. 6, pp. 5983–5994, Jun. 2020.
[27] H. Ren, S. Chen, L. Yang, and Y. Zhao, "Optimal path planning and speed control integration strategy for UGVs in static and dynamic environments," *IEEE Trans. on Veh. Technol.*, vol. 69, no. 10, pp. 10619–10629, Oct. 2020.
[28] J. W. Choi and K. Huhtala, "Constrained global path optimization for articulated steering vehicles," *IEEE Trans. Veh. Technol.*, vol. 65, no. 4, pp. 1868–1879, Apr. 2016.
[29] J. Li, G. Deng, C. Luo, Q. Lin, Q. Yan, and Z. Ming, "A. hybrid path planning method in unmanned air/ground vehicle (UAV/UGV) cooperative systems," *IEEE Trans. Veh. Technol.*, vol. 65, no. 12, pp. 9585–9596, Dec. 2016.
[30] Y. Wu, K. H. Low, and C. Lv, "Cooperative path planning for heterogeneous unmanned vehicles in a search-and-track mission aiming at an underwater target," *IEEE Trans. Veh. Technol.*, vol. 69, no. 6, pp. 6782–6787, Jun. 2020.
[31] D. González, J. Pérez, V. Milanés, and F. Nashashibi, "A review of motion planning techniques for automated vehicles," *IEEE Trans. Intell. Transp. Syst.*, vol. 17, no. 4, pp. 1135–1145, Apr. 2016.
[32] P. Raja and S. Pugazhenthi, "Optimal path planning of mobile robots: A review," *Int. J. Phys. Sci.*, vol. 7, no. 9, pp. 1314–1320, 2012.
[33] P. K. Mohanty and D. R. Parhi, "Controlling the motion of an autonomous mobile robot using various techniques: A review," *J. Adv. Mech. Eng.*, vol. 1, no. 1, pp. 24–39, 2013.
[34] S. Tang, W. Khaksar, N. Ismail, and M. Ariffin, "A. review on robot motion planning approaches," *Pertanika J. Sci. Technol.*, vol. 20, no. 1, pp. 15–29, 2012.
[35] Z. Shiller, "Off-line and on-line trajectory planning," *Motion Oper. Planning Robot. Systems*, Berlin, Germany: Springer, 2015, pp. 29–62.
[36] Y. Koren and J. Borenstein, "Potential field methods and their inherent limitations for mobile robot navigation," in *Proc. IEEE Int. Conf. Robot. Automat.*, 1991, pp. 1398–1404.
[37] B. Siciliano, L. Sciavicco, L. Villani, and G. Oriolo, *Robotics: Modelling, Planning and Control*. Springer-Verlag, London: Springer Science & Business Media, 2010.
[38] T. J. Ross, *Fuzzy Logic With Engineering Applications*. Hoboken, NJ, USA: Wiley, 2010.

Lantian Shangguan received the B.S. degree in transportation and traffic and the M.E. degree in vehicle engineering from China Agricultural University, Beijing, China, in 2012 and 2014, respectively, and the Ph.D. degree in biological and agricultural engineering from Texas A&M University, College Station, TX, USA, in 2020.

From 2016 to 2019, he was a Research Assistant with the Connected Autonomous Safe Transportation (CAST) Lab, Department of Mechanical Engineering, Texas A&M University. In 2019, he was a Research Assistant with the Biological Engineering Sensor Technologies (BEST) Lab, Department of Biological and Agricultural Engineering, Texas A&M University. His research interests include motion planning and control for autonomous (agricultural) vehicles, and safety or security enhancement for cyber physical systems.

He is currently with Intelligent Vehicle Business Unit as part of the Intelligent Driving Group, Baidu, Inc., Shenzhen, China. He leads a team focusing on decision, planning, and control algorithms for Baidu's Automated Valet Parking solution.

J. Alex Thomasson received the B.S. degree in agricultural engineering from Texas Tech University, Lubbock, TX, USA, in 1987, the M.S. degree in agricultural engineering from Louisiana State University, Baton Rouge, LA, USA, in 1989, and the Ph.D. degree in agricultural engineering from the University of Kentucky, Lexington, KY, USA, in 1997. His graduate research was focused on remote and proximal image-based sensing for agricultural applications, focusing on image analysis and sensors for the characterization of agricultural materials.

He was with the U.S. Department of Agriculture as a Research Engineer from 1989 to 1997, Mississippi State University, Mississippi State, MS, USA, as a Faculty Member from 1997 to 2004, and Texas A& M University, College Station, TX, USA, from 2005 to 2020, rising to the rank of Professor and Endowed Chair of cotton engineering, ginning, and mechanization in 2017.

Since mid-2020, he has been a Professor, the Department Head, and the Berry Endowed Chair with the Department of Agricultural and Biological Engineering, Mississippi State University. His research interests include remote and proximal sensing with imaging and nonimaging optoelectronic sensors, precision agriculture, and autonomous agricultural vehicles, with particular emphasis on characterizing and managing stresses in cotton and other crop plants during the growing season and control of postharvest processing.

Swaminathan Gopalswamy received the B.Tech. degree in mechanical engineering from the Indian Institute of Technology Madras, Chennai, India in 1987, and the M.S. and Ph.D. degrees in mechanical engineering from the University of CaliforniaBerkeley, CA, USA, in 1989 and 1991, respectively, focusing on nonlinear control theory and flight control applications.

He worked in the automotive industry for more than two decades, focusing on powertrain controls, using a model based systems engineering approach for the design and development of complex mechatronic systems.

He is currently with Texas A&M University, College Station, TX, USA. His current research focuses on autonomous vehicles, with particular emphasis on safety and new techno-business paradigms that will accelerate the safe deployment of autonomous vehicles.